

# Finesse of silicon-based terahertz Fabry-Perot spectrometer

Justin W. Cleary, Robert E. Peale  
Department of Physics, University of Central Florida, Orlando FL 32816

Ravi Todi and Kalpathy Sundaram  
Electrical Engineering and Computer Science, University of Central Florida, Orlando FL 32816

Oliver Edwards  
Zyberwear Inc., 2114 New Victor Rd., Ocoee FL 34761

## ABSTRACT

This paper considers factors that affect achievable finesse for a recently demonstrated silicon-based scanning Fabry-Perot transmission filter at millimeter and sub-millimeter wavelengths. The mirrors are formed by alternating quarter-wave optical thicknesses of silicon and air in the usual Bragg configuration. Fundamental loss by lattice and free carrier absorption are considered. Technological factors such as surface roughness, bowing, and misalignment are considered for various proposed manufacturing schemes.

**Keywords:** Fabry-Perot, terahertz, Bragg mirror, far-IR, millimeter wave, etching

## 1. INTRODUCTION

A previous paper presented design considerations and experimental results for a novel scanning Fabry-Perot spectrometer for sub-millimeter and millimeter wavelengths.<sup>1</sup> The novelty of this spectrometer was the Bragg mirrors based on silicon layers separated by air gaps. Absent technological factors such as imperfect reflecting surfaces and misalignment, finesse values exceeding 10000 were predicted at sub-millimeter wavelengths for as few as 4 periods in each mirror. Such finesse would be at least two orders of magnitude higher than has been predicted or achieved for Fabry-Perot filters based on metal mesh mirrors, which are standard practice in sub-millimeter wave airborne or satellite astronomy. A high finesse Fabry-Perot could be operated in low resonance order to achieve high resolving power and a broad free spectral range simultaneously. This would greatly simplify the pre-filter that is necessary to limit the system transmittance to a single resonance order, resulting in a simple lightweight system that might find use for defense applications.

The objective of this work was to better quantify both the fundamental and technological factors that can limit the finesse. In the usual Bragg mirror configuration, the silicon layers would have an optical thickness of one quarter of the wavelength, giving a physical thickness of  $\sim 7 \mu\text{m}$  at  $100 \mu\text{m}$  free space wavelength. Each such silicon layer would be separated by a  $25 \mu\text{m}$  gap. This paper considers the limitations posed by the achievable manufacturing tolerances. Fundamental optical losses due to free carrier and lattice absorption are also considered.

Various procedures have been considered to create quarter-wave Bragg stacks out of silicon wafers. The simplest is to separate silicon layers by mechanically independent spacers,<sup>2-5</sup> as was done in Ref. [1]. Silicon Bragg stacks have also been created by laser drilling and deep reactive ion etching.<sup>6</sup> Chemical etching and a photoresist process are considered here.

The theoretical maximum finesse is usually determined from the reflectivity of each of the cavity mirrors. Experimental finesse values are determined from the widths of the observed transmittance resonances, and they are nearly always significantly less than predicted for reasons that have been thoroughly explored.<sup>7</sup> Besides fundamental loss mechanisms, such as absorption and scattering, technological factors such as mirror-surface roughness, lack of mirror flatness (bowing), and mirror misalignment are strongly limiting technological factors.

## 2. THEORETICAL

Detailed equations used to design silicon-based Fabry-Perots and to evaluate experimental studies of such filters were presented in our previous paper.<sup>1</sup> The experimental finesse value is calculated from transmittance resonances by

$$F = \lambda / (2 \delta) , \quad (1)$$

where  $\lambda$  is the wavelength and  $\delta$  is the full-width at half-maximum transmittance resonance of the scanning Fabry-Perot. The maximum theoretical finesse for a transmission resonance in a Fabry-Perot is

$$F_R = \frac{\pi\sqrt{R}}{1-R} , \quad (2)$$

where the reflectivity  $R$  of the Bragg mirror. We refer to  $F_R$  as the reflectivity finesse. Calculation of  $R$  requires knowledge of the complex refractive index  $\eta' + i \eta''$ , where  $\eta'$  is the refractive index and  $\eta''$  is the extinction coefficient of silicon. Values for  $\eta'$  are tabulated for wavelengths out to 333  $\mu\text{m}$ ,<sup>8</sup> and we linearly extrapolate these data for wavelengths out to mm wavelengths. The extinction coefficient is then found according to

$$\eta'' = c \alpha / (2 \omega) , \quad (3)$$

where the absorption coefficient  $\alpha$  is the sum of lattice and free carrier contributions. Lattice absorption was discussed previously.<sup>1</sup> The free carrier contribution is here calculated according to<sup>9,10</sup>

$$\alpha_f = \frac{Nq^2\tau}{\epsilon_0 c \eta' m^* (1 + \omega^2 \tau^2)} , \quad (4)$$

where  $N$  is carrier concentration,  $q$  is the electron charge,  $m^*$  is the effective mass of the charge carriers, and  $\tau$  is the mean relaxation time of the charge carriers. This relation gives the well known  $\lambda^2$  dependence in the sub-mm wavelength region, where  $\omega\tau \gg 1$ . At mm wavelengths Eq. (4) approaches a constant. With resistivity and dopant identified by the silicon supplier, the carrier concentration and mobility  $\mu$  may be determined from empirical data.<sup>11</sup> The relaxation time is then determined from  $\mu$  according to

$$\tau = m^* \mu / q , \quad (5)$$

allowing numerical evaluation of Eqs. (3) and (4).

For n-type silicon, the extinction coefficient is plotted in Fig. 1 (left) for different resistivity values. In the sub-mm regime, the free carrier contribution can be small compared to the lattice contribution for resistivity  $\geq 1,000 \Omega\text{-cm}$ . In the mm-wave range, free carrier absorption always dominates, implying that the highest available resistivity is essential to achieving high finesse. We consider the values plotted in Fig. 1 (left) to be more accurate than those we previously presented in Ref. [1].

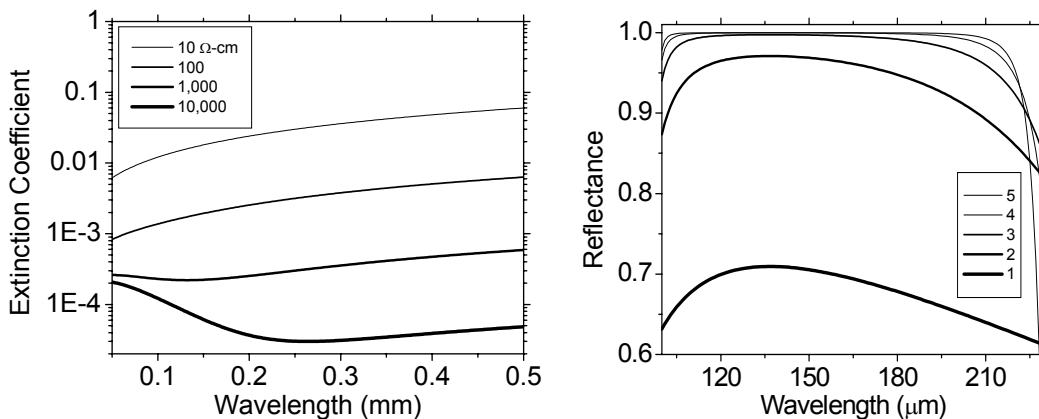


Fig. 1. (left) Total optical extinction coefficient for n-type silicon vs. wavelength and different resistivities. (right) Reflectance spectrum for a Bragg mirror composed of different numbers (legend) of 10 μm Si layers separated by 34.2 μm gaps.

Based on the new loss values, new reflectivity spectra were calculated for mirrors made from n-type 10,000 Ω-cm silicon with peak reflectivity at 136.8 μm, as plotted vs wavelength in Fig. 1 (right). Fig. 2 (left) shows that a reflectivity of 99.994% is achieved using five periods. Calculated  $F_R$  values for such mirrors are plotted in Fig. 2 (right). Due to absorption loss,  $F_R$  saturates for six periods at a value of about 78,000, so that going beyond this gives no advantage. The effect of resistivity on the Fabry-Perot resonance widths and peak transmission is essentially the same as in Ref. [1], with the conclusion that resistivity near 1,000 Ω-cm is needed for mm waves while ~ 100 Ω-cm suffices for sub-mm waves.

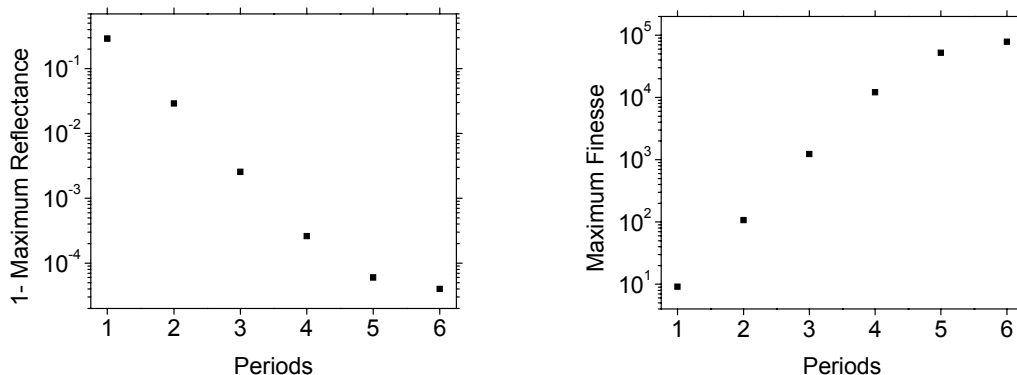


Fig. 2. (Center) Semilog plot of  $1-R_{\max}$  vs. number of periods in Bragg mirror. (Right) Calculated maximum Fabry-Perot cavity finesse using Bragg mirrors with up to 6 periods.

The experimental finesse  $F$  is reduced from the value of  $F_R$  (which already includes fundamental absorption losses) by various technological factors, according to<sup>12</sup>

$$F^{-2} = F_R^{-2} + F_D^{-2} + F_B^{-2} + F_P^{-2} + F_\theta^{-2}, \quad (6)$$

where  $F_D$  is due to mirror surface roughness,  $F_B$  is due to bowing of the mirrors,  $F_P$  is due to misalignment non-parallelism, and  $F_\theta$  is due to optical ray deviation from normal incidence. The latter factor is related to the external optical system and not specifically to technological issues regarding the manufacture of the mirrors, so that we will neglect it here. Derivations of formulas relating  $F_D$ ,  $F_B$ , and  $F_P$  were presented by Chabbal<sup>7</sup> with nearly all subsequently published discussions ultimately traceable to this paper. An alternate determination of the influence of nonuniform

mirror spacing was presented by Ulrich, Renk, and Genzel<sup>13</sup> with quantitatively the similar conclusions. Here we follow the formulation of Chabbal.

The factor  $F_B$  due to spherical bowing is determined according to

$$F_B = \lambda / (2 b) \quad , \quad (7)$$

where  $b$  is the magnitude of the bowing at the center of the mirror relative to its edges. Such bowing can occur by improper polishing (as done purposely in amateur lens making), or through thermal expansion if the edges of the mirror are clamped in a holder with different expansion coefficient. The factor  $F_P$  due to finite accuracy in adjusting the parallelism of the mirrors is given by

$$F_P = \lambda / (\sqrt{3} p) \quad , \quad (8)$$

where  $p$  is the maximum variation in distance between the two mirrors due to the tilt. The factor  $F_D$  due to surface defects is

$$F_D = \lambda / [\sqrt{(32 \ln 2)} d], \quad (9)$$

where  $d$  is the mean deviation of mirror planarity due to a gaussian distribution of defects. The scattering loss caused by such defects is ignored.

### 3. EXPERIMENTAL DETAILS

The method of forming silicon Bragg stacks in our previous experimental demonstration of a scanning Fabry-Perot spectrometer used commercial double-side polished wafers that were simply stacked using mechanically independent spacers.<sup>1</sup> In the mm-wave range, the spacers were machined brass. At sub-mm wavelengths, the spacers were formed of mylar.

A practical Bragg-mirror Fabry Perot requires a more robust monolithic mirror. Anisotropic etching of silicon wafers was explored as a means of making thin Si foils surrounded by an integrated ring of silicon as a spacer. Wafers of both <111> and <100> orientation were considered. The silicon wafers were standard cleaned, and then 500 nm of oxide was grown on them in a wet oxidation furnace at 1100 °C. The oxidized wafers were then patterned with negative photo resist to form windows for oxide etching. The back side of the silicon wafer was also protected by negative photo resist. The patterned silicon wafers were etched in buffered oxide etch solution to strip the oxide and open windows for silicon etching. After stripping the oxide within the patterned windows, the remaining photo resist was removed with acetone. Then the silicon within the windows was thinned by etching in trimethylammonium hydroxide (CH<sub>3</sub>)<sub>4</sub>NOH (TMAH). Isopropyl alcohol was added to the TMAH solution to obtain smoother surfaces. Roughness and depth of the etched surfaces was characterization using an optical profilometer.

To investigate the photoresist process, patterned 26 μm spacers of SU8 photoresist polymer were fabricated on top a silicon substrate. The spacer was characterized by optical profilometry.

### 4. RESULTS

We first summarize the results of Ref. [1]. The test of the mm-wave scanning Fabry-Perot spectrometer used 3 period Bragg mirrors and a 3.7 mm wavelength provided by a Backward Wave Oscillator. The calculated  $F_R$  value was 960, while the measured  $F$  value was 422. The test of the sub-mm wave scanning Fabry-Perot used 2 period Bragg mirrors and a 134 μm wavelength provided by a gas laser. The calculated  $F_R$  value was 100 while the measured finesse  $F$  was only 6. We next consider how the factors  $F_B$ ,  $F_D$ , and  $F_P$  might have affected those results, and we also estimate these factors for the proposed etching and photoresist processes from initial fabrication experiments and physical characterization.

Silicon wafers of 10 micron thickness are flexible and are subject to considerable distortion as a consequence of differential thermal expansion. Supposing such a wafer to be rigidly clamped in an aluminum ring gives a probable upper bound for the degree of bowing for a given temperature change. The linear expansion coefficient for silicon is<sup>14</sup>  $2.6 \times 10^{-6} \text{ K}^{-1}$ . For aluminum it is  $24 \times 10^{-6} \text{ K}^{-1}$ . The differential thermal expansion for a 1 cm diameter silicon wafer that undergoes a 20 C temperature change is then  $\sim 4 \mu\text{m}$ , which results in a bowing of the silicon  $b$  of order 100  $\mu\text{m}$ . Eq. (7) then predicts an  $F_B$  value of only 0.5 at 100  $\mu\text{m}$  wavelength. Even at 3 mm wavelength,  $F_B$  is only 15. Thus, thermal deformation may strongly degrade the total finesse  $F$ , and the manufacturing method must carefully consider this effect. In our previous demonstration,<sup>1</sup> none of the silicon layers was rigidly bound, the mechanically independent spacers were attached at their edges with flexible rubber cement, and both assembly and characterization were done in a controlled laboratory environment. Thus, there is no strong reason to suspect that  $F_B$  was the limiting factor in the experimental finesse.

The surface roughness  $d$  of commercial polished wafers, such as were used in Ref. [1], is of order 2 nm, giving  $F_D \sim 10000$  at 100  $\mu\text{m}$  wavelength and  $\sim 300000$  at 3 mm wavelength. Thus,  $F_D$  was unimportant in Ref. [1]. The situation will be similar for the photoresist process, but the situation with etched wafers is considerably different. Fig. 3 presents depth profiles for our etching experiments. Besides being very slow, etching of  $\langle 111 \rangle$  oriented wafers produced a poor surface finish with characteristic roughness  $d$  of magnitude 1  $\mu\text{m}$ . On the other hand,  $\langle 100 \rangle$  etched wafers produced a surface roughness  $d$  less than 100 nm, for which  $F_D$  is  $\sim 200$  at 100  $\mu\text{m}$  wavelength and  $\sim 6000$  at 3 mm. Thus surface roughness of etched wafers would reduce the total finesse by about 2 orders of magnitude at sub-mm wavelengths from the high values predicted on the basis of  $F_R$  alone. Still, a finesse of 200 would exceed the highest values reported for sub-mm wave Fabry-Perot spectrometers based on metal mesh.

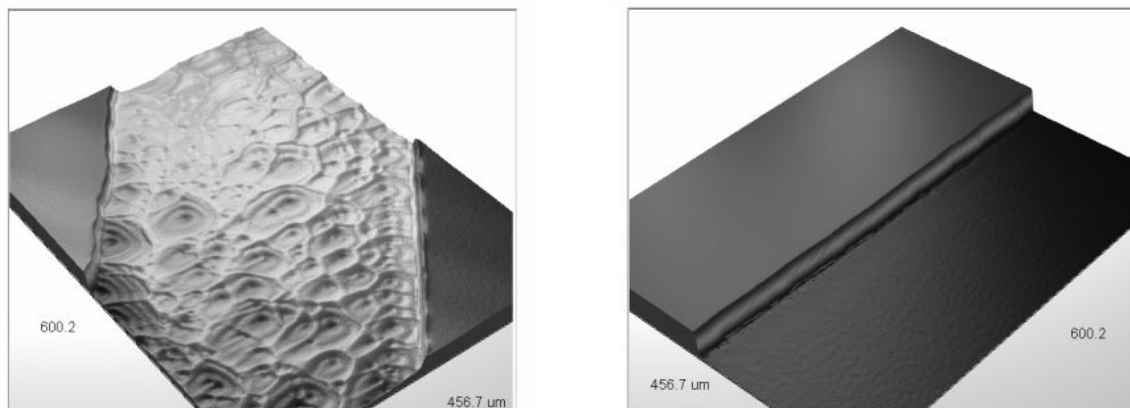


Fig. 3. (left) Depth profiling image for 60 minute patterned etch on  $\langle 111 \rangle$  oriented Si, where the etch depth produced is only  $\sim 1.2 \mu\text{m}$  and the resulting surface is rough. (right) Image for 60 minute patterned etch on  $\langle 100 \rangle$  oriented Si, where the achieved depth is  $\sim 21 \mu\text{m}$  and the surface is comparatively smooth.

The last factor we consider is  $F_p$ . In our previous mm-wave demonstration, standard off-the-shelf wafers were used. The parallelness of commercial double side polished wafers is rarely better than 1  $\mu\text{m}$  over transverse dimensions of a few cm, and this value is a measure of the minimum  $p$  value for the complete Fabry-Perot system, giving  $F_p \sim 1700$  for the mm-wave experiments. However, the predicted  $F_R$  value for the 3000  $\Omega\text{-cm}$  wafers used was only 880, so that wafer non-parallelism was unlikely to be a limiting factor in that experiment. The ultrathin 10  $\mu\text{m}$  wafers used in the experiment at 134  $\mu\text{m}$  had been prepared to a higher degree of parallelism than usual double side polished wafers. Assuming parallelism to be better than 100 nm (it was not specified or measured), gives an  $F_p$  value of  $\sim 800$ , which is very much greater than than the calculated  $F_R$  value of 100. We note that these  $F_p$  values are upper bounds, while it is unlikely that the pair of mirrors in our sub-mm wave Fabry-Perot experiment could have been aligned to better than 1  $\mu\text{m}$ , giving a more realistic  $F_p$  value of 80 for the sub-mm wave experiment. This is still much higher than the measured  $F$  value of 6. The SU8 photoresist spacers gave a surface height variation of  $\sim 1 \mu\text{m}$ , so that an FP value as low as  $\sim 80$  might be expected for a sub-mm Fabry-Perot fabricated by this method.

## 5. DISCUSSION

Table I summarizes the results presented above. The factor  $F_B$  is ignored because we do not consider it to have been important in our prior demonstration, and because we assume that the potential bowing due to differential thermal expansion can be engineered out. Likewise,  $F_\theta$  is ignored, since this relates to the entire optical system, not the manufacturing tolerances of the Fabry-Perot itself. The values given for the Ref. [1] experiment reflect the actual mirrors built. The values for the two proposed processes are somewhat speculative given that complete Bragg mirrors have yet to be constructed by either method. The  $F_P$  factors are upper bounds, since we consider only non-parallelism due to manufacturing effects, assuming that the two mirrors in the Fabry-Perot can be otherwise perfectly aligned.

Table I. Estimated finesse factors for 100  $\mu\text{m}$  (3 mm) wavelength.

	$F_R$	$F_D$	$F_P$	$F$	$F_{exp}$
Ref. [1] Experiment	100 (960), 2 (3) periods	10000 (300000)	800 (1700)	100 (610)	6 (422)
Etching process	$\sim 52000$ , 5 periods	200 (6000)	800 (1700)	190 (1600)	----
photoresist process	$\sim 52000$ , 5 periods	10000 (300000)	80 (170)	80 (170)	----

From Table I, we note that FR value limits the total finesse in the Ref. [1] experiments. That  $F_{exp} \ll F_R$  for the sub-mm wave experiment indicates that non-technological factors such as  $F_\theta$  were likely important. This suggests that if a means can be found to securely bond commercial ultra-thin wafers into a multi-layer Bragg stack, then a high finesse sub-mm wave Fabry-Perot spectrometer is possible in principle.

The etching process seems mainly limited by the resulting surface quality. Etched  $<100>$  surfaces need to be characterized by atomic force microscopy to obtain a better measure of the final surface quality. In any case, a sub-mm wave Fabry-Perot based on etched Bragg mirrors should still be competitive with the best metal mesh systems.

The photoresist process appears mainly limited by the flatness of the photoresist spacers, according to the single measurement performed here. However, additional experiments should be done to better establish the limits.

## ACKNOWLEDGMENTS

This work was supported in part by an NASA SBIR Phase I NNC06CB23C to Zyberwear, by a matching grant from the Florida High Technology Corridor program, by an ASEE summer faculty fellowship for R. E. Peale at AFRL/SNHC Hanscom AFB, and by an AFRL contract FA871806C0076.

## REFERENCES

1. J. W. Cleary, C. J. Fredrickson, A. V. Muravjov, J. B. Enz, M. V. Dolguikh, T. W. Du Bosq, R. E. Peale, W. R. Folks, S. Pandey, G. Boreman, O. Edwards, "Scanning Fabry-Perot filter for terahertz spectroscopy based on silicon dielectric mirrors," *Terahertz and Gigahertz Electronics and Photonics VI*, edited by K. J. Linden, L. P. Sadwick, *Proc. SPIE* **6472**, 64720C, 2007.
2. T. W. Du Bosq, A. V. Muravjov, R. E. Peale, and C. J. Fredricksen, "Multi-layer silicon cavity mirrors for the far-infrared p-Ge laser," *Appl. Optics* **44**, 7191-7195, 2005.
3. T. W. Du Bosq, A. V. Muravjov, and R. E. Peale, "High reflectivity intracavity Bragg mirrors for the far-infrared p-Ge laser," *Terahertz for Military and Security Applications II*, edited by R. J. Hwu, D. L. Woolard, *Proc. SPIE* **5411**, 167-173, 2004.
4. T. W. Du Bosq, E. W. Nelson, A. V. Muravjov, D. A. Walters, G. Subramanian, K. B. Sundaram, R. E. Peale, N. Tache, D. B. Tanner, C. J. Fredrickson, "Etalon, lamellar, and Bragg intracavity wavelength selecting mirrors for the far-infrared p-Ge laser," OSA meeting, *Optics in the Southeast*, Orlando, 2003.
5. R. Schiwon, G. Schwaab, E. Brundermann, M. Havenith, "Far-infrared multilayer mirrors," *Appl. Phys. Lett.* **83**, 4119-4121, 2003.

6. H. Sun, W. Shi, Z. Fu, Y. J. Ding, "Bragg reflectors and 2-D photonic crystals in the THz region," *Terahertz for Military and Security Applications III*, ed. by R. J. Hwu, D. L. Woolard, M. J. Rosker, Proc. SPIE **5790**, 104-115, 2005.
7. P. R. Chabbal, "Finesse Limite D'un Fabry-Perot Forme De Lames Imperfaites," *J. Phys. Radium* **19**, 295-300, 1958.
8. E. W. Loewenstein, D. R. Smith, and R. L. Morgan, "Optical constants of far infrared materials 2: Crystalline solids," *Appl. Optics* **12**, 398, 1973.
9. A. H. Kahn, "Theory of the Infrared Absorption of Carriers in Germanium and Silicon," *Phy. Rev.* **97**, 1647-1652, 1955.
10. Frederick Seitz, *The Modern Theory of Solids*, Dover, New York, 1987.
11. S. M. Sze, *Physics of Semiconductor Devices 2<sup>nd</sup> ed.*, Ch. 1, Sec. 1.5, Appendix G, Wiley-Interscience, New York, 1981.
12. P. Belland, J. C. Lecullier, "Scanning Fabry-Perot interferometer performance and optimum use in the far infrared range," *Appl. Optics* **19**, 1946-1952, 1980.
13. R. Ulrich, K. F. Renk, L. Genzel, "Tunable Submillimeter Interferometers of the Fabry-Perot Type," *IEEE Trans. Microwave Theory and Techniques*, **MTT-11**, 363-371, 1963.
14. Y. Okada, Y. Tokumaru, "Precise determination of lattice parameter and thermal expansion coefficient of silicon between 300 and 1500 K," *J. Appl. Phys.* **56**, 314-320, 1984.